Chenciner bubbles and hysteresis

Shuya Hidaka[†], Naohiko Inaba[‡], Kyohei Kamiyama[†], Munehisa Sekikawa[*], and Tetsuro Endo[†]

[†] Department of Electronics and Bioinformatics, Meiji University, 214–8571 Kawasaki, Japan
[‡] Organization for the Strategic Coordination of Research and Intellectual Property, Meiji University, 214–8571 Kawasaki, Japan
[*] Department of Mechanical and Intelligent Engineering, Utsunomiya University, 321–8585 Utsunomiya, Japan
Email: ce41083@meiji.ac.jp, naohiko@yomogi.jp

Abstract—This study investigates quasi-periodic bifurcations and Arnol'd resonance webs generated in a coupled delayed logistic map. Because a single delayed logistic map generates an invariant closed curve corresponding to a two-dimensional torus in vector fields via a Neimark-Sacker bifurcation, the coupled delayed logistic map can exhibit an invariant torus corresponding to a three-dimensional torus in vector fields. The Lyapunov analysis is conducted, and it is clarified that Chenciner bubbles are generated by saddle-node bifurcations and Neimark-Sacker bifurcations. Inevitably, Chenciner bubbles are accompanied with hysteresis.

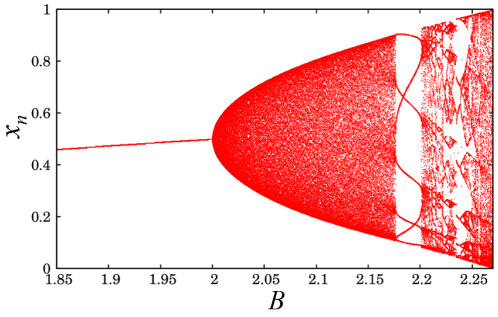

Figure 1: One-parameter bifurcation diagram of a delayed logistic map.

1. Introduction

The partial and complete synchronizations of three or higher frequency quasi-periodic oscillations have recently been studied extensively [1–26]. Vitolo *et al.* clarified that two types of bifurcation routes from a two-dimensional torus to a three-dimensional torus [10] exist. One is a quasi-periodic Hopf (QH) bifurcation, and the other is a quasi-periodic saddle-node (QSN) bifurcation. The QH bifurcation is also called a quasi-periodic Neimark-Sacker (QNS) bifurcation [22, 24] because Hopf did not analyze maps. The Arnol'd resonance web is a phenomenon that was discovered and defined by Broer *et al.* [1] in the numerical analysis of a map, where regions generating invariant closed curves (ICCs) corresponding to two-dimensional tori in vector fields extends in many direction in the invariant torus generating region like a web in a two-parameter bifurcation diagram.

As far as we know, the web like structure of partial and complete synchronization regions of a three-dimensional torus was first experimentally denoted by Linsay and Cumming in 1989 [2] who carried out circuit experiments on two coupled relaxation oscillators with a periodic forcing. They introduced the term "fractal devil's cobweb." In 1991, Baesens *et al.* analyzed torus maps, and introduced the concept of *partial* and *full mode locking* [3], and they called the complex bifurcation structure mode locking webs.

The bifurcation analysis of Arnol'd resonance webs have recently been advancing rapidly. The observation of Arnol'd resonance webs are usually performed by Lyapunov analysis. Kuznetsov *et al.* investigated quasi-periodic bifurcations generated in maps and ordinary differential equations by employing an advanced computational power [6–8, 19]. Kuznetsov *et al.* analyzed Arnol'd resonance webs generating up to five-dimensional tori in a discrete-time dynamics [6], and Emelianova *et al.* investigated ensemble of van der Pol oscillators [8]. Arnol'd resonance webs in maps have similar aspects to those of ordinary differential equations. Furthermore, the Arnol'd resonance web is observable in laboratory measurements [21].

In this study, we investigate a bifurcation structure of Chenciner bubbles [23], which is periodic-solution-generating region around which two thicker two-torus Arnol'd tongues intersect. Inevitably, hysteresis is observed around Chenciner bubbles. Our numerical results show that a two-torus Arnol'd tongue and a periodic solution coexist. We hypothesize that the hysteresis occurs because of a subcritical Neimark-Sacker bifurcation and a QSN bifurcations. The image of the bifurcation structure is illustrated. Furthermore, the complex basin boundaries are observed between the two-dimensional torus and the periodic solutions. This study is the first report that investigates hysteresis of Chenciner bubbles.

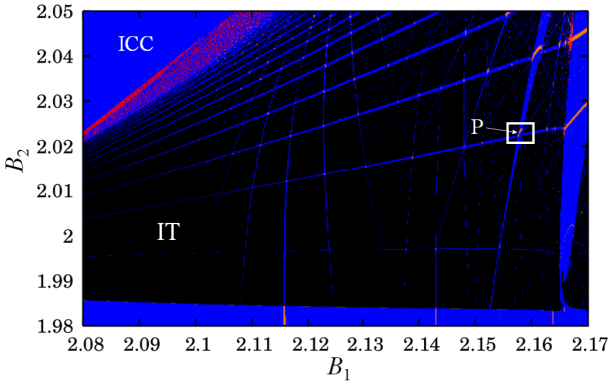

Figure 2: Global view of the bifurcation diagram.

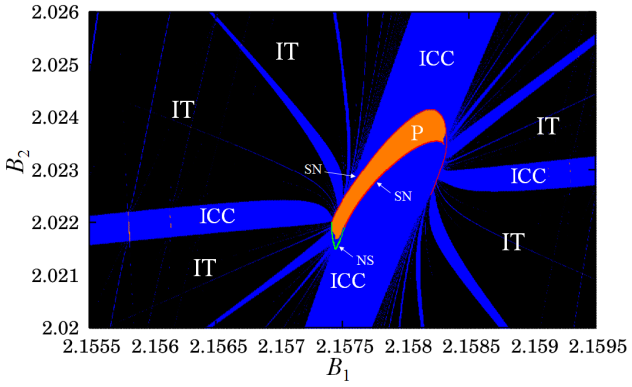

Figure 3: Magnified view of Fig. 2.

2. Two-coupled delayed logistic map and Arnol'd resonance webs

We recall the fundamental properties of the delayed logistic map. The delayed logistic map is expressed by the following form:

$$\begin{aligned} x_{n+1} &= y_n, \\ y_{n+1} &= By_n(1 - x_n). \end{aligned} \tag{1}$$

This map exhibits an ICC owing to a Neimark-Sacker bifurcation. Since it is a simple diffeomorphism, the Neimark-Sacker bifurcation point is manually calculated, and it occurs at $B = 2$. Figure 1 shows the one-parameter diagram.

In this study, we analyze a coupled delayed logistic map in the following form:

$$\begin{aligned} x_{n+1} &= y_n, \\ y_{n+1} &= B_1 y_n(1 - x_n) + \varepsilon_1 w_n \\ z_{n+1} &= w_n, \\ w_{n+1} &= B_2 w_n(1 - z_n) + \varepsilon_2 y_n. \end{aligned} \tag{2}$$

Since Eq. (1) generates a Neimark-Sacker bifurcation at $B = 2$, Eq. (2) generates an invariant torus near $B_1 \simeq 2$ and $B_2 \simeq 2$ if ε_1 and ε_2 are sufficiently small.

The procedure in deriving the Lyapunov exponents are as follows.

$$\begin{aligned} \lambda_1 &\simeq \frac{1}{N}\sum_{j=M+1}^{M+N} \ln \|DF_j e_1^j\|, \\ \lambda_1 + \lambda_2 &\simeq \frac{1}{N}\sum_{j=M+1}^{M+N} \ln \|DF_j e_1^j \times DF_j e_2^j\|, \\ \lambda_1 + \lambda_2 + \lambda_3 &\simeq \frac{1}{N}\sum_{j=M+1}^{M+N} \ln \|DF_j e_1^j \times DF_j e_2^j \times DF_j e_3^j\|, \\ \lambda_1 + \lambda_2 + \lambda_3 + \lambda_4 &\simeq \\ &\frac{1}{N}\sum_{j=M+1}^{M+N} \ln \|DF_j e_1^j \times DF_j e_2^j \times DF_j e_3^j \times DF_j e_4^j\|, \end{aligned} \tag{3}$$

where DF_j is a Jacobian matrix of F on F^j and e_i ($i = 1, 2, 3,$ and 4) are orthonormal bases obtained by the procedure in Ref. [27]. We use sufficiently large M and N. In actual calculation, we employ $M = 1,000,000$ and $N = 1,000,000$, and we consider that λ_i is perceived as exact zero if the following inequality holds:

$$\lambda_i = 0 \text{ if } |\lambda_i| < \frac{1}{100,000}. \tag{4}$$

In the following discussion, we set $\varepsilon_1 = 0.01$ and $\varepsilon_2 = 0.02$. Figure 2 shows a global bifurcation diagram around $B_1 \simeq 2$ and $B_2 \simeq 2$, which is obtained via Lyapunov analysis presented in Ref. [27]. In the figure, black, blue, orange, and red regions indicate invariant tori, ICCs, periodic solution-generating regions, and chaos-generating regions, respectively. Inside the region generating an invariant torus, regions generating ICCs extend like a web in many direction as shown in Fig. 2, which can be called an Arnol'd resonance web. At the intersection of thicker two ICC-generating regions, a periodic solution generating region can be observed. Such regions are called Chenciner bubbles [23]. The magnified view of Fig. 2 is shown in Fig. 3. Complex bifurcation structure is observed in Fig. 3. In the figure, a green curve and red curves denote a Neimark-Sacker bifurcation line, and saddle-node bifurcation lines, which are derived by a shooting algorithm proposed in Ref. [28]. Note that the bifurcation boundaries obtained by Lyapunov analysis and by the shooting algorithm do not fit completely. Therefore, we present highly magnified view of Fig. 4. From Figs. 4(a) and (b), inevitable hysteresis is observed. The coexisting attactors at Q ($B_1 = 2.15745$, $B_2 = 2.02165$) in Fig. 4 are presented in Fig. 5. We hypothesize that the bifurcation structure is cause by a subcritical Neimark-Sacker bifurcation and QSN bifurcation. The situation is illustrated in Fig. 6. In the figure, a stable periodic point and a stable ICC are illustrated by the solid lines, and unstable ones are illustrated by the broken lines.

Next, we investigate the initial condition boundary,

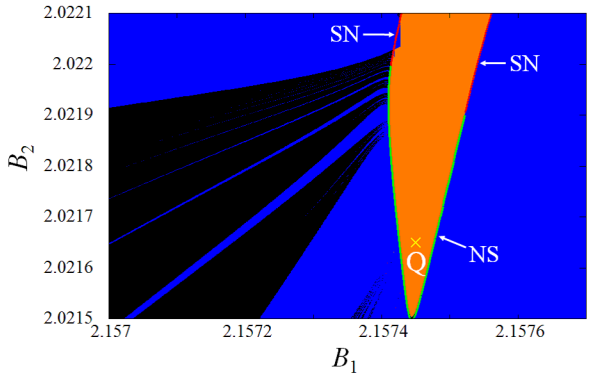

(a)

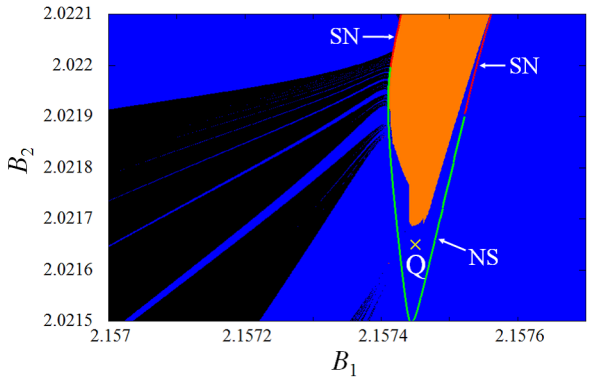

(b)

Figure 4: Highly magnified view of Fig. 3. (a) Bifurcation parameter B_2 is traced from top to bottom. (b) Bifurcation parameter B_2 is traced from bottom to top.

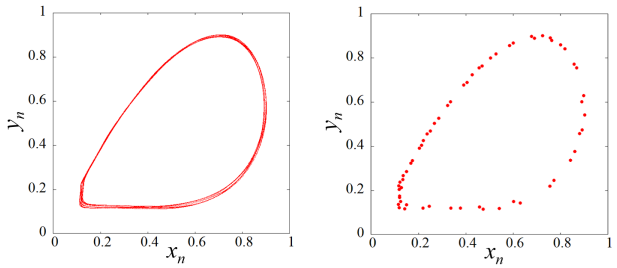

(a) (b)

Figure 5: Coexisting attractors at Q in Fig. 4. (a) Stable two-dimensional torus. (b) Periodic solution.

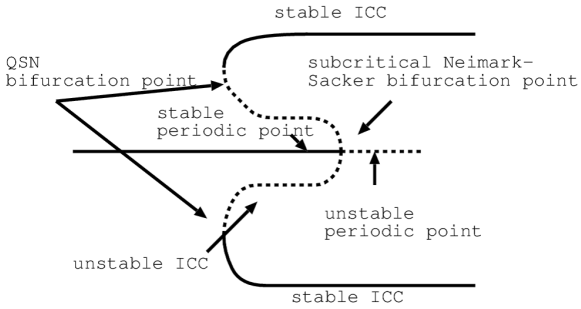

Figure 6: Expected bifurcation structure.

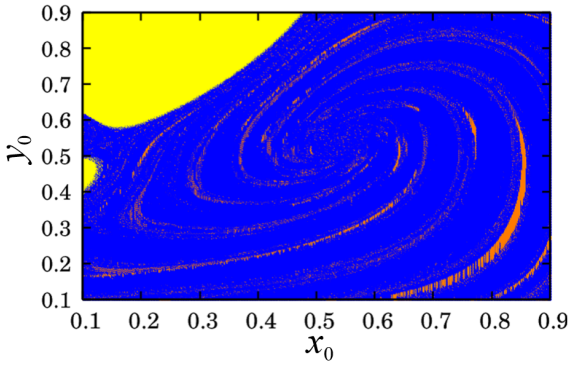

Figure 7: Fractal basin boundary at Q in Fig. 4 ($z_0 = 0.8$, $w_0 = 0.8$).

which is illustrated in Fig. 7. In the figure, blue, and orange zones indicate regions where an ICC and a periodic point are stable. In addition, yellow denotes the region that results in the initial conditions representative of diverging solutions. The fractal basin is observed.

3. Conclusion

This study analyzed quasi-periodic bifurcations observed in a coupled delayed logistic map. Complex bifurcation such as Chenciner bubbles accompanied hysteresis, and fractal basin boundaries were observed. Since the dynamics of the present study is a simple diffeomorphism, the phenomena demonstrated in this study could be universal.

References

[1] H. Broer, C. Simó, R. Vitolo, The Hopf-saddle-node bifurcation for fixed points of 3D-diffeomorphisms: the Arnol'd resonance web, Bull. Belg. Math. Soc. Simon Stevin 15 (2008) 769–787.

[2] P.S. Linsay, A.W. Cumming, Three-frequency quasiperiodicity, phase locking, and the onset of chaos, Physica D 40 (1989) 196–217.

[3] C. Baesens, J. Guckenheimer, S. Kim, R.S. MacKay, Three coupled oscillators: mode locking, global bifurcations and toroidal chaos, Physica D 49 (1991) 387–475.

[4] A.P. Kuznetsov, S.P. Kuznetsov, I.R. Sataev, L.V. Turukina, About Landau-Hopf scenario in a system of coupled self-oscillators, Phys. Lett. A 377 (2013) 3291–3295.

[5] N.V. Stankevich, J. Kurths, A.P. Kuznetsov, Forced synchronization of quasiperiodic oscillations, Communications in Nonlinear Science and Numerical Simulation 20 (2015) 316–323.

[6] A.P. Kuznetsov, Y.V. Sedova, Low-dimensional discrete Kuramoto model: Hierarchy of multifrequency quasiperiodicity regimes, Int. J. Bifurc. Chaos 24 (2014) 1430022.

[7] Y.P. Emelianova, A.P. Kuznetsov, I.R. Sataev, L.V. Turukina, Synchronization and multi-frequency oscillations in the low-dimensional chain of the self-oscillators, Physica D 244 (2013) 36–49.

[8] Y.P. Emelianova, A.P. Kuznetsov, L.V. Turukina, I.R. Sataev, N.Y. Chernyshov, A structure of the oscillation frequencies parameter space for the system of dissipatively coupled oscillators, Communications in Nonlinear Science and Numerical Simulation 19 (2014) 1203–1212.

[9] H. Broer, C. Simó, R. Vitolo, Hopf saddle-node bifurcation for fixed points of 3D-diffeomorphisms: Analysis of a resonance 'bubble,' Physica D 237 (2008) 1773–1799.

[10] R. Vitolo, H. Broer, C. Simó, Quasi-periodic Bifurcations of Invariant Circles in Low-dimensional Dissipative Dynamical Systems, Regular and Chaotic Dynamics 16 (2011) 154–184.

[11] V.S. Anishchenko, M.A. Safonova, U. Feudel, J. Kurths, Bifurcation and transition to chaos through three-dimensional tori, Int. J. Bifurc. Chaos 4 (1994) 595–607.

[12] V. Anishchenko, S. Nikolaev, J. Kurths, Bifurcational mechanisms of synchronization of a resonant limit cycle on a two-dimensional torus, Chaos 18 (2008) 037123.

[13] V.S. Anishchenko, S.M. Nikolaev, J. Kurths, Synchronization mechanisms of resonant limit cycle on two-dimensional torus. Rus. J. Nonlin. Dyn. 4 (2008) 39–56.

[14] S. Hidaka, N. Inaba, M. Sekikawa, and T. Endo, Bifurcation analysis of four-frequency quasi-periodic oscillations in a three-coupled delayed logistic map, Phys. Lett. A 379 (2015) 664–668.

[15] K. Kyohei, N. Inaba, M. Sekikawa, and T. Endo, Bifurcation boundaries of three-frequency quasi-periodic oscillations in discrete-time dynamical system, Physica D 289 (2014) 12–17.

[16] V. Anishchenko, S. Astakhov, T. Vadivasova, Phase dynamics of two coupled oscillators under external periodic force, Europhys. Lett. 86 (2009) 30003.

[17] V. S. Anishchenko, S. V. Astakhov, T. E. Vadivasova, A. V. Feoktistov, Numerical and experimental study of external synchronization of two-frequency oscillations, Nelin. Dinam. 5 (2009) 237–252.

[18] A.P. Kuznetsov, I.R. Sataev, L.V. Tyuryukina, Synchronization of quasi-periodic oscillations in coupled phase oscillators, Tech. Phys. Lett. 36 (2010) 478–481.

[19] A.P. Kuznetsov, I.R. Sataev, and L.V. Turukina, On the road towards multidimensional tori, Commun Nonlinear Sci Number Simulat 16 (2011) 2371–2376.

[20] Y.P.Emelianova, A.P.Kuznetsov, and L.V.Turukina, Quasi-periodic bifurcations and " amplitude death " in low-dimensional ensemble of van der Pol oscillators, Physics Letters A 378 (2014) 153–157.

[21] M. Sekikawa, N. Inaba, T. Tsubouchi, K. Aihara, Novel bifurcation structure generated in piecewise-linear three-LC resonant circuit and its Lyapunov analysis, Physica D 241 (2012) 1169–1178.

[22] M. Sekikawa, N. Inaba, K. Kamiyama, K. Aihara, Three-dimensional tori and Arnold tongues, Chaos 24 (2014) 013017.

[23] P. Ashwin, Boundary of Two Frequency Behaviour in a System of Three Weakly Coupled Electronic Oscillators, Chaos Sol. Frac. 9 (1998) 1279–1287.

[24] K. Itoh, N. Inaba, M. Sekikawa, T. Endo, Three-torus-causing mechanism in a third-order forced oscillator, Prog. Theor. Exp. Phys. 2013 (2013) 0903A02.

[25] N. Inaba, M. Sekikawa, Y. Shinotsuka, K. Kamiyama, K. Fujimoto, T. Yoshinaga, T. Endo, Bifurcation scenarios for a 3D torus and torus-doubling, Prog. Theor. Exp. Phys. 2014 (2014) 023A01.

[26] F. Takens, F.O.O. Wagener, Resonances in skew and reducible quasi-periodic Hopf bifurcations, Nonlinearity 13 (2000) 377–396.

[27] I. Shimada, T. Nagashima, A numerical approach to ergodic problem of dissipative dynamical system, Prog. Theor. Phys. 61 (1979) 1605–1616.

[28] H. Kawakami, Bifurcation of periodic responses in forced dynamic nonlinear circuits: Computation of bifurcation values of the system parameters, IEEE Trans. Circuits Syst. CAS-31 (1984) 248–260.